Development of the sheet-pile foundation; A new seismic resistant foundation

S. Higuchi[1], H. Nishioka[2], K. Tanaka[1], M. Koda[2], J. Hirao[3], N. Tsuji[3], M. Tateyama[2] and T. Matsuda[3]

[1] Technical Research Institute of OBAYASHI Co., Japan
[2] Railway Technical Research Institute, Japan
[3] Civil Engineering Technology Div., OBAYASHI Co., Japan
Email: higuchi.shunichi@obayashi.co.jp

ABSTRACT :
The authors have proposed the sheet-pile foundation (SPF, hereafter) as a new foundation type. This foundation has advantages as follows; 1) Wider applicability to various soil conditions than the shallow foundations, 2) Minor impact to the environment with construction work, 3) More economical than the pile foundations in terms of cost. In this paper, seismic tests conducted to investigate the fundamental characteristics of the sheet-pile foundation during the earthquake for the development of the design method are presented.

KEYWORDS:
Foundation, Sheet-pile, Seismic design, Horizontal loading test, Shake table test

1. INTRODUCTION

Recently, development of construction methods for densely populated urban area is emphasized in Japan. For example, in order to ease traffic congestion, railroads are re-laid on viaducts. For this project, structures are usually constructed very close to existing structures, and the space allowed for construction work is limited. In addition, it is required to reduce costs, as well as minimizing the impact to the environment, such as noise, vibration and disposals from construction work.
Sheet-pile Foundation (SPF, hereafter), which combines the footing and sheet-piles, proposed as a new foundation form (Koda et al. 2003, Nishioka et al. 2004) is one solution. Because of the confinement of the ground is increased by the sheet-piles, both bearing capacity and horizontal resistance of the SPF are improved compared to those of the shallow foundation. Therefore, the applicability became wider than that of the shallow foundations. For example, SPF can be adopted on the loose sandy ground to which the pile foundation has been usually applied. The construction cost of SPF is almost the same as that of the shallow foundation and more competitive than that of the pile foundation. On the other hand, since the pile work is not necessary, it can avoid various disadvantages of pile foundation, such as noise, vibration and the disposal of surplus soil. Figure 1 shows an outline of the sheet-pile foundation compared with the shallow foundation and the pile foundation.
In this paper, a series of static loading tests (laboratory and full-scale in the field) and centrifuge tests carried out for the purpose to evaluate the performance of the sheet-pile foundation are presented and discussed.

2. HORIZONTAL LOADING TESTS

2.1. Outline of model ground and foundations

A model ground was prepared in a rigid container with dry sand. The model was a two-dimensional in plane strain condition. The sand container's side walls were made of transparent acrylic plates to allow observation of the deformation of the ground. In order to reduce friction between the acrylic plate and sand, rubber membranes were pasted on acrylic plate with grease. Target points were marked on the rubber membrane for measuring displacement of the ground by an image processing system. Table 1 summarizes the conditions of the model ground. The relative density Dr of the model ground was controlled by the height of the sand hopper to 90% or 60%. The model footing was made of aluminum block of 100 mm in n width B, and placed on the model ground surface.

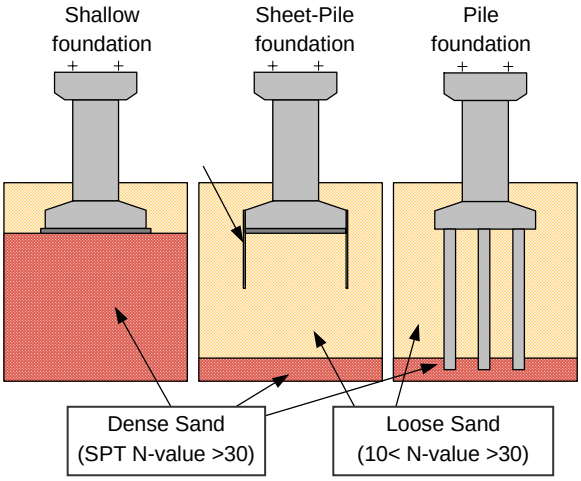

Figure1 Outline of the sheet-pile foundation

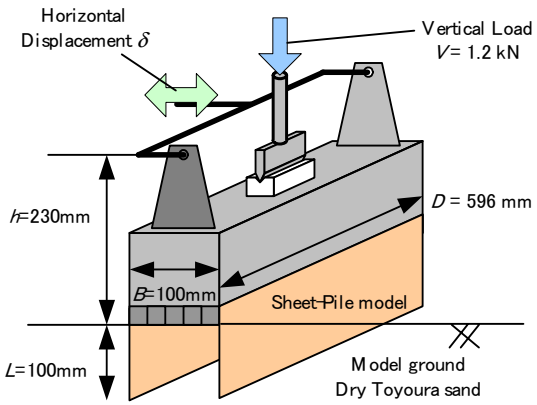

Figure2 Outline of horizontal reciprocal loading test.

Model sheet-pile was made of phosphor bronze plates with 0.2 mm thickness, and they were pressed to concavo-convex form. The length L that was installed into the ground was 100 mm (L/B=1.0) or 50 mm (L/B=0.5). The value of β_L shown in Eq.1 of the model sheet-piles was the same grade as that of prototype.

$$\beta L = \sqrt[4]{k_h D / 4EI} \cdot L \qquad (2.1)$$

where β: Characteristic value of pile (1/m), k_h: Coefficient of horizontal subgrade reaction (kN/m^3), D: Width of sheet-piles (m), EI: Flexural rigidity of sheet-pile (kNm^2), L: Length of sheet-pile (m).
Table 2 summarizes specifications of the model sheet-piles.

Table 1 Conditions of modeled ground

Ground dimension (W × H × D)	2000 mm × 580 mm × 600 mm
Material of ground	Dry Toyoura sand
Dry unit weight γ_d	γ_d = 16.2 kN/m^3 (D_r = 90%) γ_d = 15.1 kN/m^3 (D_r = 60%)
Lubricated layer	Rubber membrane (t=0.2mm) with Grease (10μm)

Table 2 Specifications of model sheet-piles

	Prototype TYPE IV	Modeled sheet-pile
Thickness	15.5 mm	0.2 mm
Height of concavo-convex form	340 mm	1.5 mm
Width of Footing B	4.8 m	100 mm
Width of sheet-piles D	4.8 m	596 mm
Young's modulus E	200 kN/mm^2 (Steel)	110 kN/mm^2 (Phosphor bronze)
Geometrical moment of inertia I	1.28×10^{-3} m^4	42.9 mm^4
Coefficient of horizontal subgrade reaction k_h	78,600 kN/m^3 (Sand N = 30)	45,700 kN/m^3 (D_r=90%)
Length L	4.8 m (L/B=1.0) 2.4 m (L/B=0.5)	100 mm (L/B=1.0) 50 mm (L/B=0.5)
β L	3.74 (L/B=1.0)	3.42 (L/B=1.0)

2.2. Test procedures

In order to simulate the effects of inertia force by the earthquake, the horizontal loading tests were conducted. The horizontal loads were applied to the bridge pier top.
An outline of the tests is shown in Figure 2. The horizontal displacement was applied with a screw jack statically and cyclically at a height of 230mm from the footing model bottom that was corresponding to the bridge pier top. The vertical load P_v=1.2 kN was applied to the pier top simultaneously by an air cylinder, which was about 10% of the bearing capacity of the shallow foundation previously tested on the dense ground model.

Table 3 Cases of horizontal loading tests

Case	Density of ground	Foundation Form
HD1	D_r=90% (Dense)	Shallow foundation
HL1	D_r =60% (Medium dense)	Shallow foundation
HL2		Sheet-pile foundation *L/B*=0.5
HL3		Sheet-pile foundation *L/B*=1.0

2.3. Test results

The relations between the horizontal load P and displacement δ at the top of pier are shown in Figure 3 and Figure 4. Figure 3 shows hysteresis curves, and Figure 4 shows skeleton curves, which connected the turning points on each loading cycles together. The SPF (Case-HL2, HL3) has higher horizontal resistance than that of shallow foundations (Case-HD1, HL1). Since the loop of the hysteric curve of the SPF is larger than that of the shallow foundation, it is clear that the hysteric damping of the SPF is larger than shallow foundations. In addition, the residual horizontal displacement of the SPF was almost negligible after the experiment.

The settlement characteristic is another important function of the railway structure. Figure 5 shows settlements of footings when the horizontal displacement reached to the peak in each cycle. Settlements became larger as the increase of horizontal displacement in all cases. Although the shallow foundation on the medium dense ground (Case-HL1) had large settlement of more than 10% of footing width, the SPF on the same ground model (Case-HL2, HL3) has only small settlements, which are as same as that of shallow foundation on the dense ground (Case-HD1). Therefore, it is clear that the sheet-piles restrained the settlement.

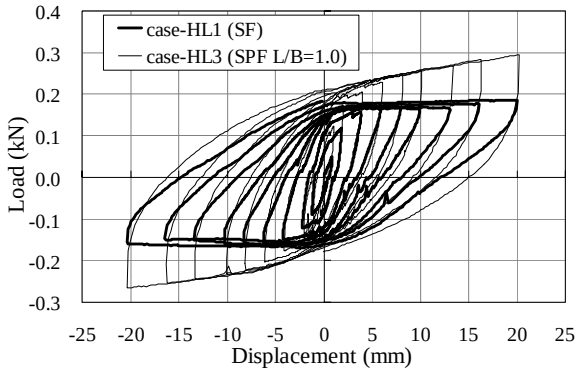

Figure 3 Hysteresis curves of P-δ relationship test

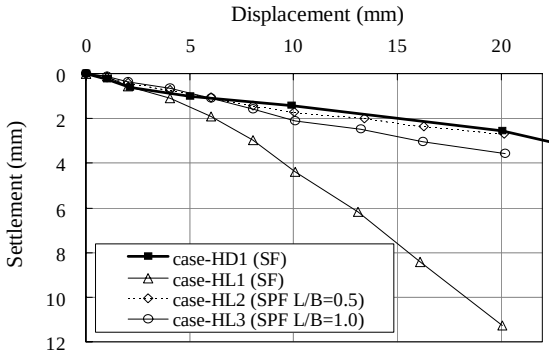

Figure 5 Skeleton curves of settlements

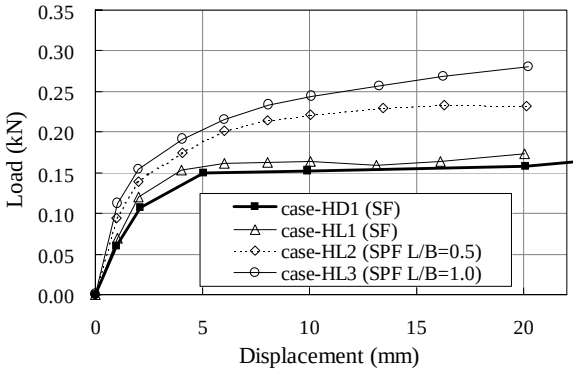

Figure 4 Skeleton curves of P-δ relationship

a) Case-HL1
Shallow foundation

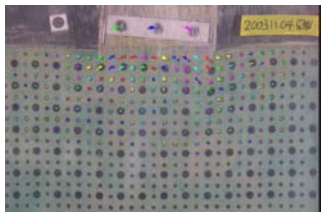

b) Case-HL2
Sheet-pile foundation
(L/B=1.0)

Photo 1 Displacement computed by the Image Processing System when horizontal displacement reaches 20mm. (Dr=60%)

Photo 1 shows the deformation of the ground in two cases (Case-HL1 and HL2), computed by the image processing system previously described. The lines in the figures show the locus of each target point until the horizontal displacement at the top of pier reaches 20mm. The deformation of the ground was observed in a large area around the model footing. In the case of the shallow foundation (Case-HL1), the ground failed like a

circular slip in the limited area shallower than 50mm on both sides of the footing. It is seen that the deformation of the ground around the footing spreads outward direction. On the other hand, in the case of the SPF (Case-HL2), the horizontal deformation of the ground is restrained by the sheet-piles.

3. CENTRIFUGE TESTS

3.1. Outline of the centrifuge models

Because of the stress dependent physical properties of ground materials, centrifuge shake table tests were conducted to simulate actual characteristics of the SPF during earthquake event. Centrifuge tests were carried out under a 25g centrifugal acceleration, therefore, the model structures were scaled as 1/25, as shown in Figure 6. A 9m high viaduct with 5m square footing was selected as the prototype (Photo 2). Sheet-pile was also scaled in this experiment except connections as shown in Figure 7. Sheet-pile length and ground density are chosen as parameters of this experiment. Table 4 summarizes the conditions of the model and ground. Shake table tests were carried out utilizing the input motions as shown in Table 5.

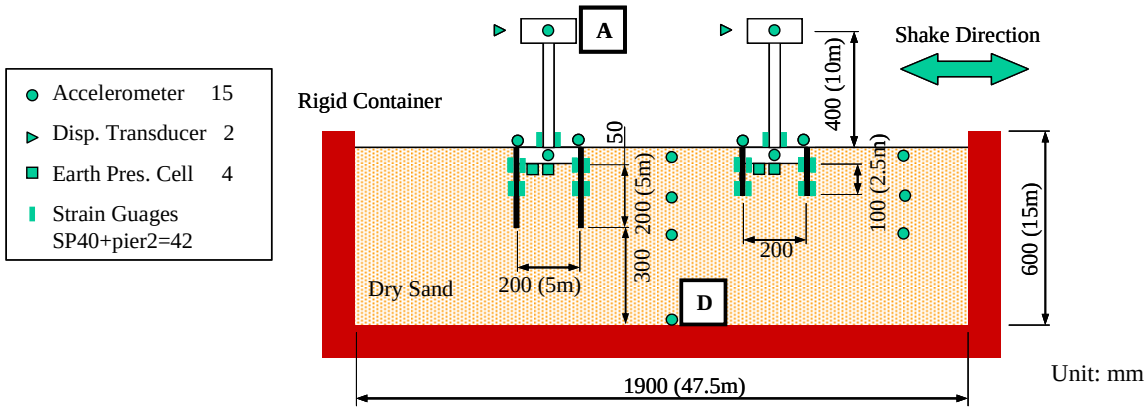

Figure 6 (a) Centrifuge setup

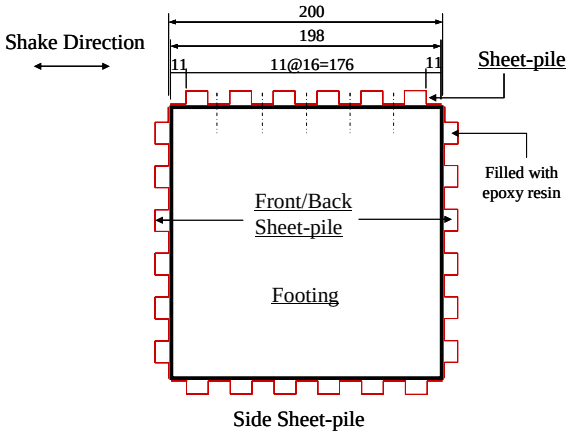

Figure 6 (b) Plan view of the footing

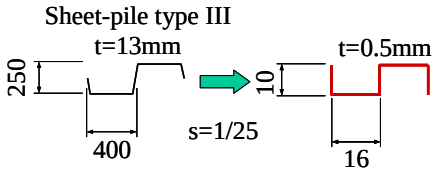

Figure 7 Model Sheet-pile

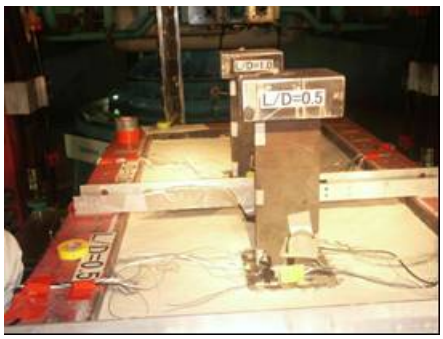

Photo 2 Model structure and ground

3.2. Test results

Distribution of the vertical self load between the sheet-piles and the footing bottom after the centrifuge acceleration process are summarized in Table 6. It is seen that larger self weight is shared by the sheet-piles on the cases of either the sheet-pile length become longer or the ground became denser.

Predominant period of the ground-structure system analyzed by the transfer functions (A/D in Figure 6) during a small event (white noise motion; Peak Acceleration=0.02g in prototype) are summarized in Table 7. This shows the initial stiffness of the SPF is larger than that of the shallow foundations, and mainly influenced by the

ground condition.

Skelton curves, which consists of relations between the horizontal response acceleration α(g) and the response displacement of the pier top δ (mm), on the shallow foundation and the sheet-pile foundations (L/B=1.0 and 0.5) at the dense ground are shown in Figure 8. These curves are found with sinusoidal input motion tests. Yield acceleration α_y of the SPF with L/B=1.0 is 0.8g, and this is twice as large as that of the shallow foundation on the same ground, of which α_y is 0.4g. α_y of the SPF with L/B=0.5 is also improved as 0.6g. This means with installing the sheet-piles in the ground, seismic performance of the shallow foundation can be largely improved, and the performance is affected by the length of the sheet-piles.

Yield accelerations α_y are also compared in Table 8, in the case of the medium dense ground. α_y of the SPF with L/B=1.0 is 0.6g in this case, and this is twice as large as that of the shallow foundation, of which the α_y is 0.3g, as proportional to the dense ground cases.

Table 4 Summary of test conditions

Case	1-1	1-2	1-3	2-1	2-2
Foundation type	Shallow foundation	SPF	SPF	Shallow foundation	SPF
Ground condition	Dense （Dr=90% : Vs=200m/s）			Medium dense（Dr=60%, Vs=180m/s）	
Sheet-pile length	-	1.0B	0.5B	-	1.0B

Note : B is the footing width

Table 5 Summary of input motions for the shake table tests

Item	Summary	Purpose
Sinusoidal motion	f=1.2Hz with 25 cycles	Investigating the basic dynamic characteristics of the SPF
Earthuake motion	A standard seismic motion, L2-spectral 1, prepared for the raylway structures by RTRI	Investigating the performance of the SPF during the earthquake event

Table 6 Vertical self load distribution after the centrifuge acceleration process

Case	1-1	1-2	1-3	2-1	2-2
Foundation type	SF	SPF	SPF	SF	SPF
Ground	Dense			Medium dense	
Sheet-pile	-	1.0B	0.5B	-	1.0B
Vertical pressure (kPa)	300	160	200	300	130
Vertical load distribution (Footing : SP)	-	1 : 0.87	1 : 0.5	-	1 : 1.3

Note : SF is the shallow foundation; SP is the sheet-pile

Table 7 Predominant period of ground-structure system measured at the small shake event

Case	1-1	1-2	1-3	2-1	2-2
Foundation type	SF	SPF	SPF	SF	SPF
Ground	Dense			Medium dense	
Sheet-pile	-	1.0B	0.5B	-	1.0B
Predominant Period (s)	0.66	0.50	0.51	0.68	0.55

Table 8 Yield accelerations (Medium dense ground)

Case	2-1	2-2
Foundation type	SF	SPF
Sheet-pile length	-	1.0B
α_y (g)	0.3	0.6

Figure 9 shows the stress time histories of the sheet-pile installed perpendicular to the shake direction during the shake event utilizing the actual earthquake motion summarized in Table 5 with its PA=0.45g at shake table. Both axial and bending stress components are far smaller than its yield limit (240MPa) during the severe earthquake event. This means the sheet-pile is not a critical member on the seismic design of the SPF.

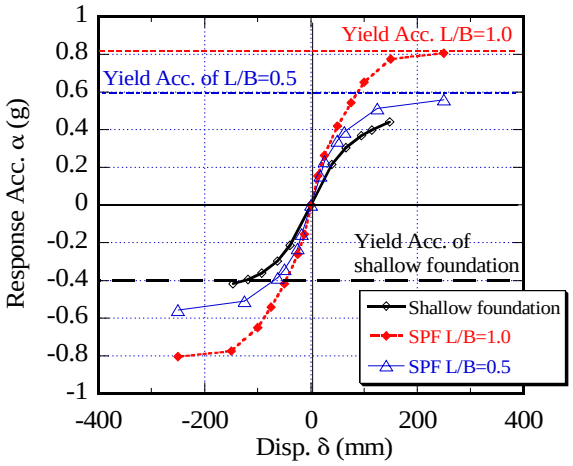

Figure 8 Load-displacement skelton curves of tested foundations (Dense ground)

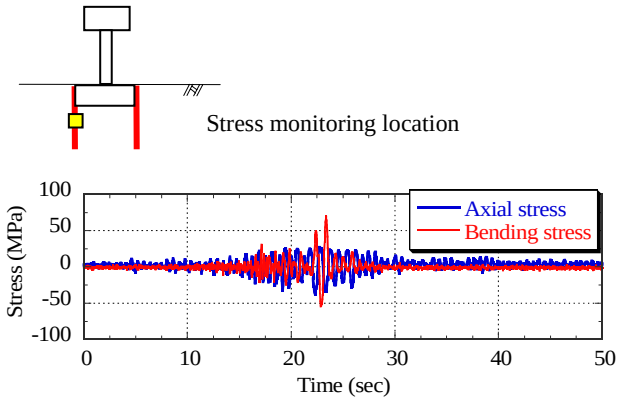

Figure 9 Stress time histories of sheet-pile

3.3. Bearing mechanism of the SPF

As it was seen, seismic performance of the SPF is largely improved compared with the shallow foundation. Therefore, the bearing mechanism of the SPF against the seismic action will be discussed in this section. Bearing mechanism against the rocking motion of the SPF is investigated utilizing the force equilibrium around the footing defined as eq. (3.1). Schematic drawings are illustrated in Figure 10, as well.

$$M_{SP} = \Sigma M_s + (N_{sp}{}^{T} - N_{sp}{}^{C}) \cdot B/2 + (M_{out}{}^{C} + M_{out}{}^{T}) \qquad (3.1)$$

Here,
M_{SP}: Resistant moment against the rotation of the footing by sheet-piles
M_s: In-plane bending moment by the side sheet-piles
$N_{sp}{}^{C}$: Axial force of the sheet-pile at the front side of the footing (Compression side)
$N_{sp}{}^{T}$: Axial force of the sheet-pile at the back side of the footing (Tension side)
$M_{out}{}^{C}$: Bending moment of the front side sheet-pile
$M_{out}{}^{T}$: Bending moment of the back side sheet-pile
B: Width of the footing

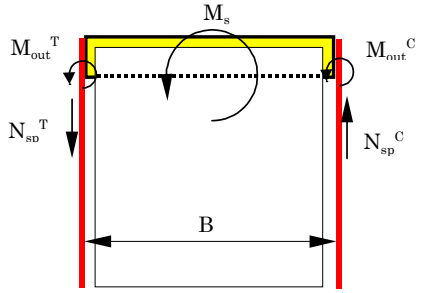

Figure10 Force equilibrium around the footing in terms of rotation of the SPF

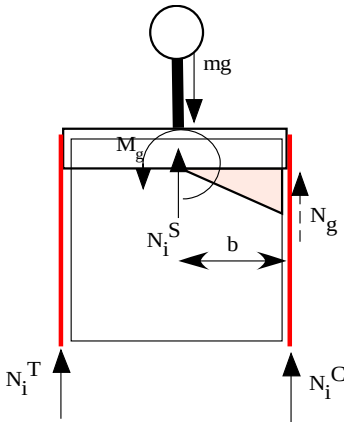

Figure 11 Schematic drawing of the rotation resistance from the ground reaction

On the other hand, the rotation resistance from the ground reaction under the footing against the rocking motion is estimated by assuming all vertical components can be supported by the vertical resistance of the front side sheet-pile as its axial force, as shown in Figure 11. Therefore, total vertical force from the ground reaction N_g and the resistant moment by the ground M_g can be calculated as follows.

$$N_g = mg - \sum N_i \tag{3.2}$$

Here,
mg: Mass of the superstructure x Centrifugal acceleration
$\sum N_i$: Sum of the vertical force of sheet-piles

$$M_g = N_g \cdot b \tag{3.3}$$

Here,
b: B/2

Therefore, total resistant moment against the rotation around the footing is defined as eq. (3.4).

$$M_{RSPF} = M_{SP} + M_g \tag{3.4}$$

Time histories of the action moment calculated from the inertia force of the structure and the resistant moment defined as eq. (3.4) are shown in Figure 12. Action moment around the footing center M_A is calculated as follows.

$$M_A = \sum m_i \alpha_i l_i \tag{3.5}$$

Here,
m_i: mass of the superstructure, pier and footing
α_i: Measured response acceleration
l_i: Arm from the center of the footing

Resistant moment is calculated by eq. (3.1) utilizing the forces measured by strain gauges on the sheet-piles. The resistant moment by the ground M_g is calculated at limited time section, as illustrated in Figure 12. Calculation results show there is good matching between M_{RSPF} and M_A. Therefore, it is confirmed that the calculation assumption was suitable. Since the calculation assumption of the bearing mechanism is reasonable, share of each reaction component against rotation can be analyzed. According to the calculation example of Figure 12, about 1/3 of the resistant moment is shared by M_g (Ground reaction component), and 2/3 is shared by M_{SP} (Sheet-pile reaction component).
Detailed analysis on the sheet-pile reaction component is carried out as shown in Figure 13. At the time step shown in the Figure 13, it is found that 86% of the resistant moment is shared by the axial resistance of the front/back sheet-piles. Only 5% is shared by the flexure resistance of the front/back sheet-piles, and rest 9% are shared by the rotation resistance by the side sheet-piles.

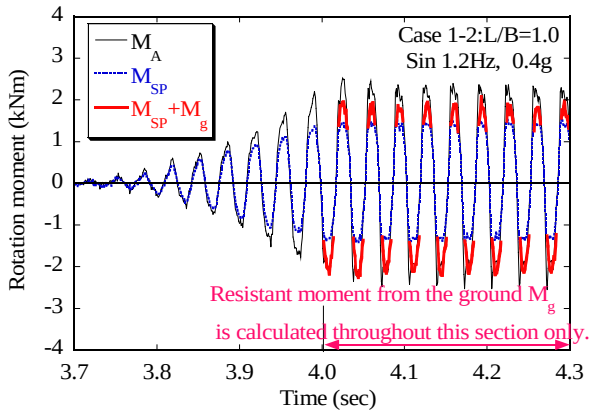

Figure 12 Time histories of the action moment and the resistant moment

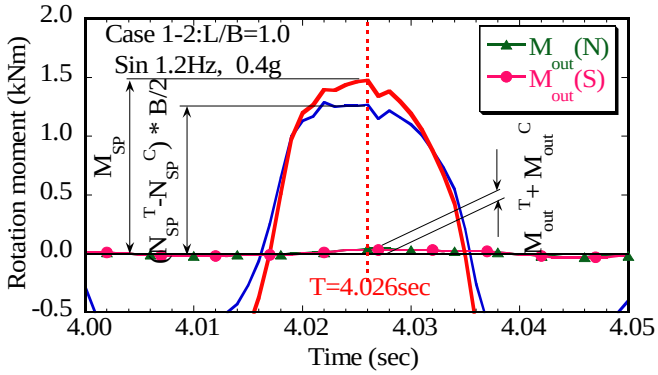

Figure 13 Time histories of each resistant moment component of M_{SP}

4. FULL-SCALE FIELD TEST

4.1. Outline of full-scale models

Aiming at practical use, the full-scale field tests were conducted in Kawagoe-City, Japan.The test setup and the models are shown in Photo 3. The surface diluvial clay (Kanto loam), with a thickness of 5m, is laid on the gravel layer. These models have a 3.6m square footing, 6m high pier. The sheet-pile's length is 3.6m, the same as the width of the footing. Therefore, the tips of the sheet-piles were not installed into the gravel layer.

4.2. Horizontal static loading test

The horizontal static loading tests were conducted by pulling the tops of two models to each other by a hydraulic jack. At first, the shallow foundation was pulled by the sheet-pile foundation. Next the sheet-pile foundation was pulled by the shallow foundation reinforced by the ground anchor.

The P-δ relation of each case is shown in Figure 14. The ratio of the horizontal resistance of the sheet-pile foundation against that of the shallow foundation was about four. This ratio is larger than that obtained by the laboratory test.

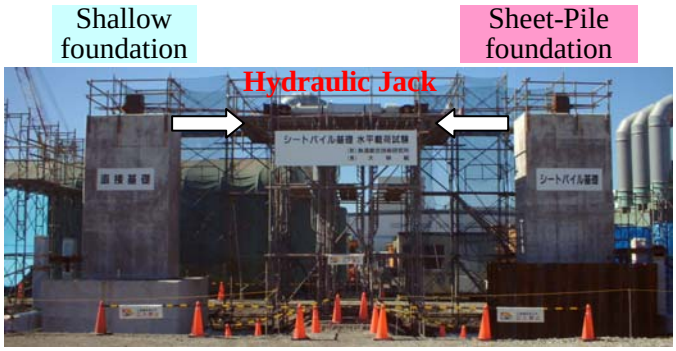

Photo 3 Test setup and full-scale models

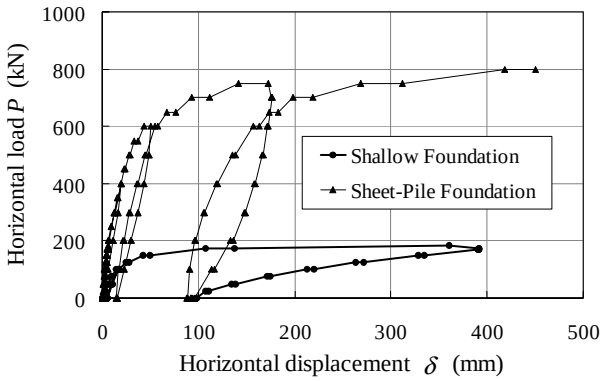

Figure 14 P-δ relationships of the models after loading

5. CONCLUSION

Followings were found from a series of tests.

1. The seismic performances of the sheet-pile foundation are greatly improved compared with those of the shallow foundation.
2. Performance of the sheet-pile foundation is influenced by both sheet-pile length and ground condition.
3. Sheet-pile is not a critical member on the seismic design of the SPF.
4. Bearing capacity of the SPF is calculated by assuming the force equilibrium around the footing.
5. Most resistant moment of the SPF is shared by the axial resistance of the front/back sheet-piles.

Based on the above test results, a guideline of design and construction of the sheet-pile foundation was published by the Railway Technical Research Institute, Japan, and several actual projects were realized so far. Because of its excellent performance and cost competitiveness, application of the sheet-pile foundation may increase in future.

REFERENCES

Koda, M., et al. (2003) The Proposal of Sheet-Pile Foundation Combining a Footing with Sheet-Piles (in Japanese), **TSU-CHI-TO-KISO, Vol. 51, No. 11**, pp.8-10

Nishioka, H., et al. (2004) A Series of Static Loading Tests of Modeled Sheet-Pile Foundation Combining Footing with Sheet-Piles on Sand, Proceeding of 15th Southeast Asian Geotechnical Society Conference, pp.199-204, Bangkok, Thailand.